

Synthesis of smart fluids for the efficient removal of residual oil from subsurface

Ch. Ntente^{1,2}, A. Strekla^{1,3}, M. Theodoropoulou¹, C.D. Tsakiroglou^{1,*}

¹Foundation for Research and Technology Hellas - Institute of Chemical Engineering Sciences (FORTH/ICE-HT), 26504 Patras, Greece

²University of Patras, Department of Chemistry, 26504 Patras, Greece

³University of Patras, Department of Physics, 26504 Patras, Greece

* Corresponding author: E-mail: ctsakir@iceht.forth.gr,
Tel +30 2610 965212, Fax: +30 2610 965223

Abstract

Aqueous solutions of polyphenols extracted from the leaves of plants are used to synthesize and stabilize aqueous suspensions of iron oxide nanoparticles by green chemistry routes. The interfacial properties and wetting properties of nano-colloids are measured to assess their capacity to generate stable Pickering emulsions. The rheological properties of emulsions are measured, and their stability is inspected by observing the phase separation (macro-scale) and measuring the drop size distribution (micro-scale). The capacity of emulsions to remove residual oil from soils is evaluated with visualization tests of drainage / primary imbibition / secondary imbibition performed on a glass-etched pore network for an oil / aqueous solution system. In each test, the transient changes of the fluid saturation along with the pressure drop across the porous medium are measured and correlated with dimensionless parameters, such as the capillary number and viscosity ratio.

Keywords: *iron oxide nanoparticles (IONPs), interfacial tension, wettability, oil displacement, soil remediation*

1. INTRODUCTION

The remediation of oil spills is an urgent global challenge due to their devastating impacts on the environment and human health [1]. Conventional methods for oil spill remediation, such as mechanical recovery and chemical dispersants, have drawbacks and limitations, including potential harm to marine life and ecosystems. Therefore, alternative and environmentally-friendly approaches are needed for efficient oil spill remediation [2].

One promising approach is the use of smart fluids synthesized via green synthesis with iron oxide nanoparticles. Iron oxide nanoparticles (IONPs) are attractive materials for environmental remediation due to their unique magnetic properties, high surface area, and stability [3,4]. Green synthesis with plant extracts is a sustainable and eco-friendly method for producing iron oxide nanoparticles [5]. IONPs can decrease the interfacial tension of oil and water, which can lead to more stable Pickering emulsions [6-8].

Several studies have demonstrated the potential of smart fluids synthesized via green synthesis with iron oxide nanoparticles for the efficient removal of residual oil from subsurface environments. In these 'greener' processes, plant extracts were used for the synthesis of nanoparticles through biosynthetic routes which involve primarily the extraction of polyphenols, which are natural polymers acting as reducing agents and stabilizers [9-11]. In summary, the synthesis of smart fluids via green synthesis with iron oxide nanoparticles is a promising approach for the efficient removal of residual oil from subsurface environment.

In this work, aqueous solutions of polyphenols are extracted from parsley leaves and mixed with a ferric chloride hexahydrate solution to produce IONPs suspensions. An ultrasound probe is used for the production of stable oil-in-water emulsions by mixing the suspensions with n-decane. The performance of the emulsions as agents for the efficient removal of residual oil from subsurface, is assessed with secondary imbibition tests, performed on a transparent glass-etched pore network, after having completed a drainage / imbibition cycle, by using as oil phase a synthetic one of controlled viscosity which was prepared by mixing paraffin oil with n-decane. A comparative analysis of the displacement efficiency of Pickering emulsions enabled us to classify them, in terms of their rheological properties.

2. MATERIALS AND METHODS

2.1 Synthesis of iron oxide nanoparticles (IONPs) suspensions and emulsion preparation

For the preparation of parsley extract, 1000 mL of triple distilled water (3D - water) was heated on a hot plate, and when the temperature reached at 80 °C, 50 g of parsley leaves was added in water, and left for 60 min, under stirring. Then, the mixture was withdrawn from the hot plate, left to equilibrate to ambient conditions, filtrated under vacuum on 4 µm and 2.5 µm pore size filters (Whatman) and centrifuged at 10000 rpm for 10 min (Heraeus Megafuge-16) to separate the liquid extract from the solid residue. The total polyphenol concentration (TPC) of the extract was measured in terms of gallic acid equivalent (g/L GAE), using the Folin-Ciocalteu method [12] and UV-Vis spectroscopy (Shimadzu UV-1900).

The synthesis of iron oxide nanoparticles (IONPs) was achieved by adding 0.1 M FeCl₃ solution in the polyphenol extract (PPH), at a volume ratio of 2:1 [13]. The colour change of the solution to dark brown certified the end of the reaction. The pH was measured with a pH-meter (CONSORT C830), adjusted to 6.0, and the suspension was placed in a refrigerator for further use.

The preparation of emulsions was done by mixing 20 mL of IONPs suspension with 10 mL of oil (n-decane) at a volume ratio 2:1 for 10 min by using an ultrasound probe (Hielscher, UP400St). The synthetic oil was prepared by mixing paraffin oil (Labkem, Spain) with n-decane (Sigma – Aldrich) at volume ratio 4:1 [14].

2.2 Characterization of IONPs suspensions and emulsions

Suspensions of IONPs were prepared at four iron concentrations 0.25, 0.5, 0.75 and 1.0 g/L. The particle size distribution, and ζ-potential of IONPs suspensions were measured with Dynamic Light Scattering -DLS (Zetasizer Nano System, Malvern) after having diluted each suspension at volume ratio 1:50 with 3DW.

The static surface tension of the suspensions, as well their interfacial tension with n-decane and synthetic oil were measured at 25°C on a Sigma 702 (KSV Instruments) tensiometer by using the DuNouy Ring method.

The static contact angles were measured by placing drops of aqueous phase, surrounded by air or oil, on a glass surface under a stereoscope (Nikon) and capturing the images with an HY-2307 CMOS camera (Hayear) connected via USB with PC and equipped with image capturing software.

The stability of Pickering emulsions was inspected macroscopically, by observing the phase separation as a function of time, and microscopically, by a CCD video camera (Micropublisher 6, Photometrics-Teledyne).

2.3. Visualization tests

Immiscible displacement tests were performed on a glass pore network model (Figure 1), to assess the capacity of IONP-stabilized emulsions to enhance the recovery of residual oil entrapped in the pore network after a primary drainage (displacement of 3-distilled water (3DW) by synthetic oil at rate $q=0.08$ mL/min), and primary imbibition (displacement of oil by 3DW at rate, $q=0.2$ mL/min). During this secondary imbibition step the emulsion displaces the residual oil at flow rate $q=0.2$ mL/min. Each displacement step started at the point that the previous step was completed, so that the oil saturation varied continuously with time. At each series of displacement tests, images were captured every 20 s by a CCD video camera (Panasonic AW-E300E). The absolute pressure was measured with two pressure transmitters (SGM, Electrosystems)(Figure 1) properly connected with a data acquisition system (ADAMS-4561 & ADAMS-4117, Advantech). Recorded snap-shots of the flow pattern were processed with image analysis software (ImageJ) to determine the gradual variation of residual oil saturation.

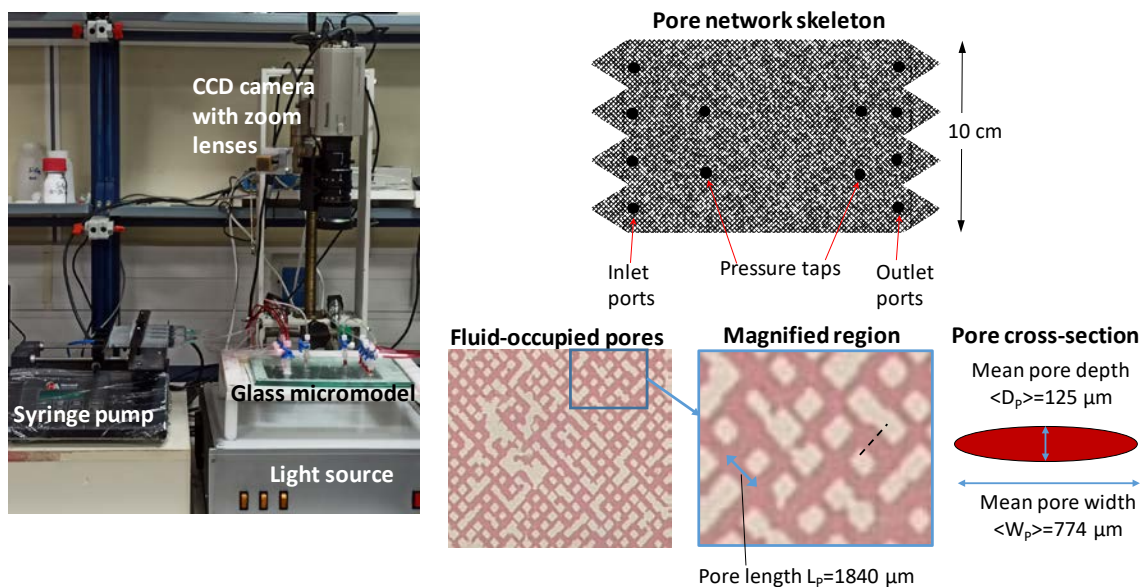


Figure 1. Experimental setup and micromodel morphology.

3. RESULTS AND DISCUSSION

3.1 Physicochemical and interfacial properties of aqueous suspensions

The polyphenol concentration in PPH extract was measured by Folin-Ciocalteu method and estimated $\sim 2.0 - 3.0$ g/L GAE, while its pH was found 6.5. Moreover, the surface tension of PPH extract was found equal to 45.3 ± 0.13 mN/m, whereas the PPH extract / n-decane, and PPH extract / synthetic oil interfacial tensions, all measured at 25°C , were found equal to 36.8 and 48.2 mN/m, respectively. The physicochemical, wetting, and interfacial properties of nanoparticle suspensions as functions of IONP concentration are shown in Table 1, Table 2, and Figure 2, respectively.

The IONP suspensions are stable, and the nanoparticle sizes exhibit a narrow size distribution (Table 1). The air/IONP suspension and oil/IONP suspension contact angle vary ($50^\circ - 75^\circ$) over the intermediate wetting range (Table 2). The surface tension of suspensions is a clearly decreasing function of IONP concentration (Figure 2) while the interfacial tension of aqueous IONP suspensions with oils is a weakly decreasing function of IONP concentration (Figure 2).

Table 1. Physicochemical properties of aqueous suspensions.

Aqueous suspension	Particle size distribution		ζ -potential (mV)
	$\langle D_p \rangle$ (nm)	σ_p (nm)	
Parsley extract, $C_{\text{PPH}}=3.0$ g/L	58.77	3.4	-11.3
IONPs, $C_{\text{Fe}}=0.25$ g/L	18.17	17.9	-28.5
IONPs, $C_{\text{Fe}}=0.5$ g/L	32.67	15.4	-29.2
IONPs, $C_{\text{Fe}}=0.75$ g/L	24.36	11.5	-10.3
IONPs, $C_{\text{Fe}}=1.0$ g/L	15.69	5.5	-25.1

Table 2. Wetting properties of aqueous suspensions.

Aqueous suspension	Air/water contact angle		Oil/water contact angle	
	$\langle \theta_{\text{aw}} \rangle$ ($^\circ$)	$\sigma_{\theta_{\text{aw}}}$ ($^\circ$)	$\langle \theta_{\text{ow}} \rangle$ ($^\circ$)	$\sigma_{\theta_{\text{ow}}}$ ($^\circ$)
Parsley extract, $C_{\text{PPH}}=3.0$ g/L	73.95	2.86	69.59	1.61
IONPs, $C_{\text{Fe}}=0.25$ g/L	52.39	7.95	48.85	7.49
IONPs, $C_{\text{Fe}}=0.5$ g/L	54.57	2.95	51.82	2.58
IONPs, $C_{\text{Fe}}=0.75$ g/L	64.00	3.18	58.98	3.61
IONPs, $C_{\text{Fe}}=1.0$ g/L	63.33	4.63	60.72	3.17

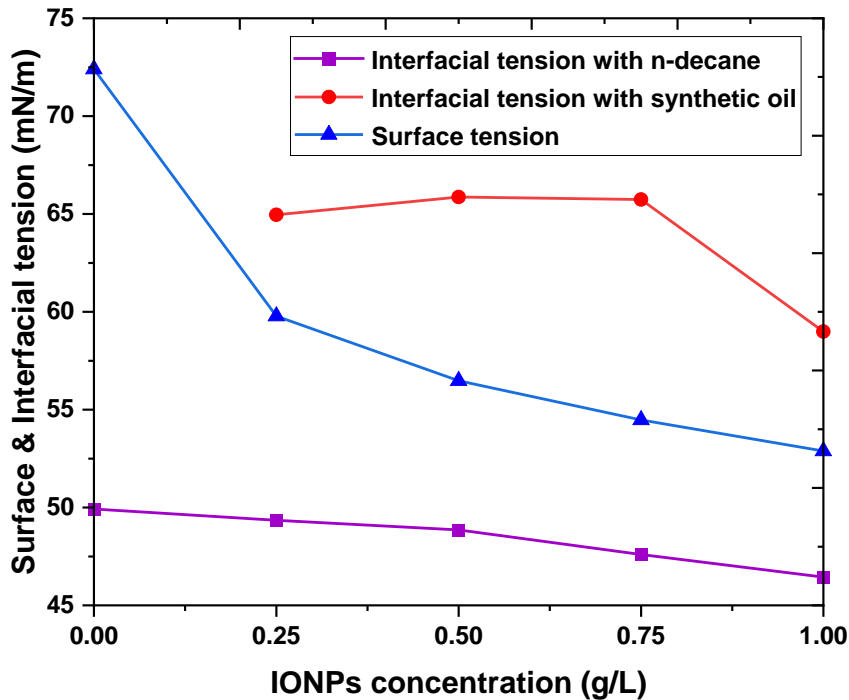


Figure 2. Interfacial properties of aqueous IONPs suspensions

3.2 Emulsion characterization

Macroscopically, examining the relative volume of each phase as function of time, all emulsions appear comparable stability, with the emulsified phase occupying 50-60% of the total volume 3hrs after their preparation (Figure 3). Rheological measurements (Figure 4) show all Pickering emulsions are shear-thinning fluids which are fitted satisfactorily with the extended power law model:

$$\mu = \mu_{inf} + (\mu_1 - \mu_{inf})\dot{\gamma}^{n-1} \quad (1)$$

where $\dot{\gamma}$ is the shear rate, μ_{inf} is the asymptotic value of viscosity as the shear rate tends to infinity, μ_1 is the viscosity at $\dot{\gamma} = 1 \text{ s}^{-1}$, and n is a power law exponent. The higher the values of μ_1 , μ_{inf} , the more viscous the emulsion. The lower the exponent n , the sharper the reduction of viscosity at increasing shear rates (Figure 4).

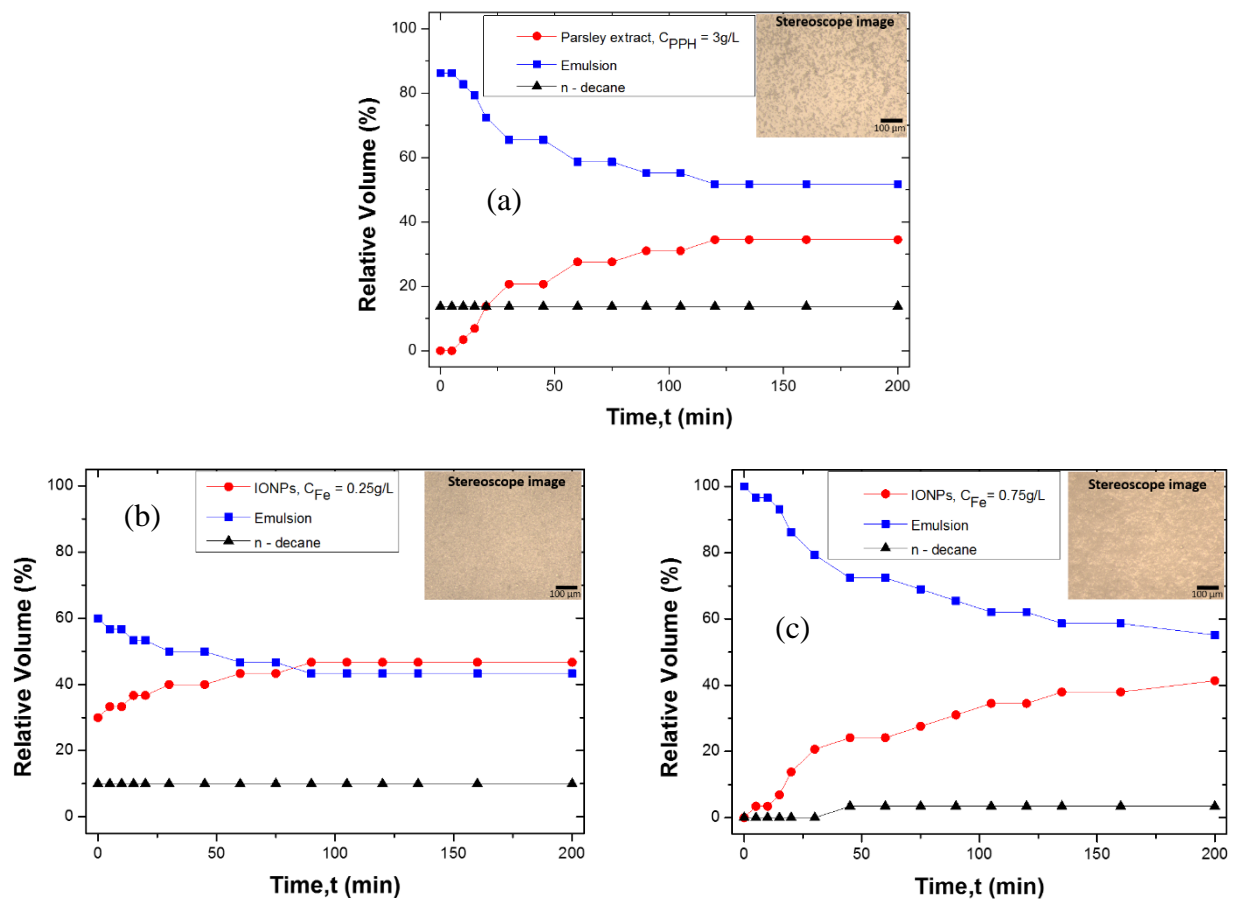


Figure 3. Transient response of the relative volume of the various phases of emulsions.
 (a) Aqueous phase: parsley extract, $C_{PPH}=3.0\text{g/L}$.
 (b) Aqueous phase: IONPs, $C_{Fe}=0.25\text{g/L}$. (c) Aqueous phase: IONPs, $C_{Fe}=0.75\text{g/L}$.

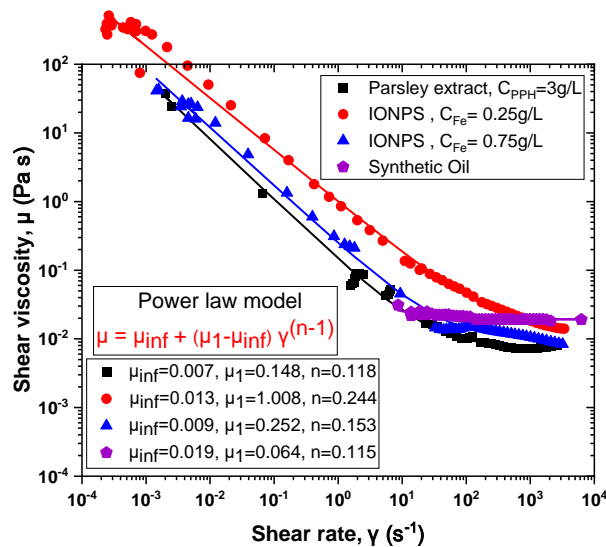


Figure 4. Shear viscosity of Pickering emulsions and synthetic oil, fitted with the extended power law model.

3.3 Visualization tests

Successive images of the primary drainage/primary imbibition /secondary imbibition cycles for the most effective Pickering emulsion (IONP with $C_{Fe}=0.25$ g/L) are shown in Figure 5. In addition, the corresponding transient response of the oil saturation and pressure drop across a central region of the porous medium are shown in Figures 6, 7 and 8 for the three emulsions tested. The highest oil recovery efficiency of secondary imbibition was achieved with the highest values of viscosity ratio and capillary number, favouring the frontal drive flow pattern (Figure 5c). The strong shear thinning viscosity of displacing fluid during the secondary imbibition is reflected in the high amplitude of the pressure drop fluctuations (Figure 7a, 8a).

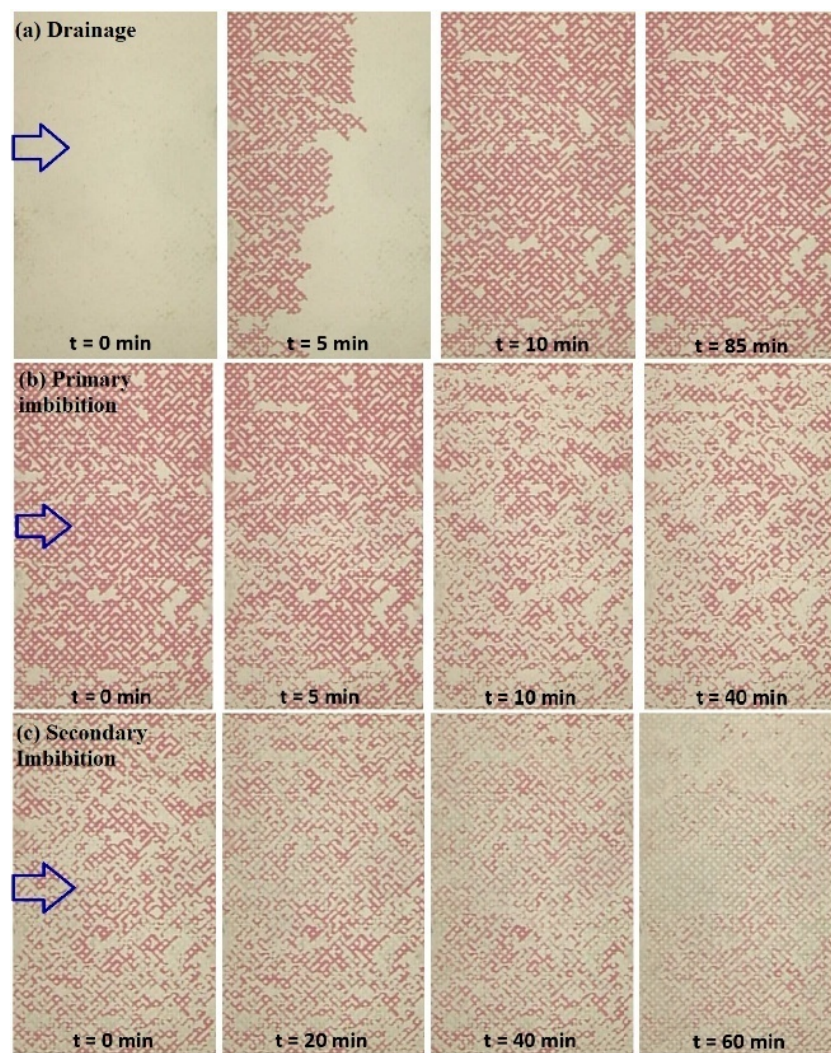


Figure 5. (a) Displacement of 3D-water by synthetic oil ($\mu=0.026$ Pa s). (b) Displacement of synthetic oil by 3D-water. (c) Displacement of residual synthetic oil by Pickering emulsion (aqueous suspension=IONPs with $C_{Fe}=0.25$ g/L; oil phase: *n*-decane; volume rate 2:1).

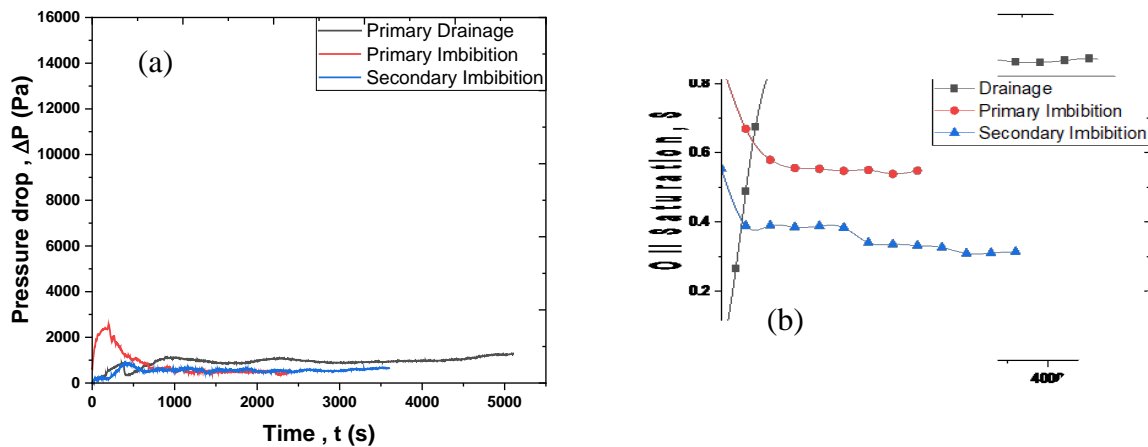


Figure 6. Transient response of (a) pressure drop, and (b) oil saturation, as a function of time. Pickering emulsion of parsley extract, $C_{PPH}=3\text{g/L}$, was injected at the secondary imbibition step.

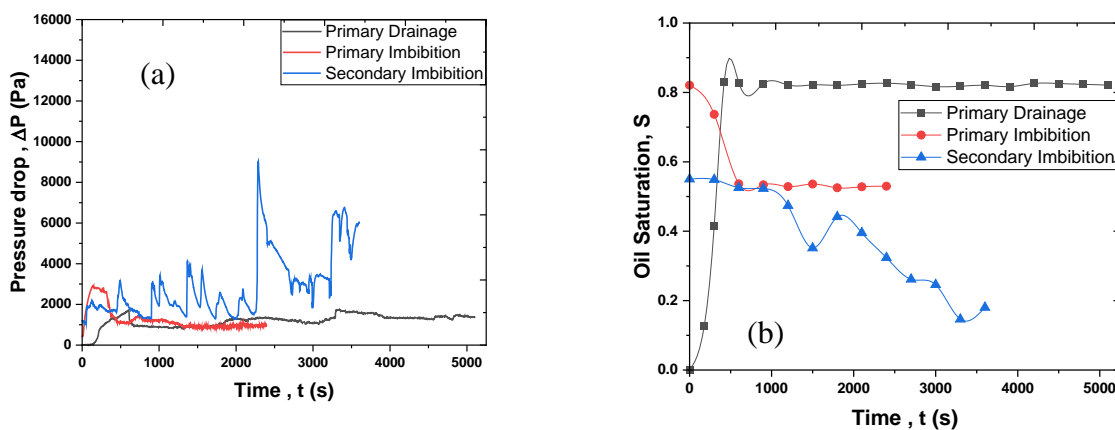


Figure 7. Transient response of (a) pressure drop, and (b) oil saturation, as a function of time. Pickering emulsion of IONPs suspension, $C_{Fe}=0.25\text{g/L}$, was injected at the secondary imbibition step.

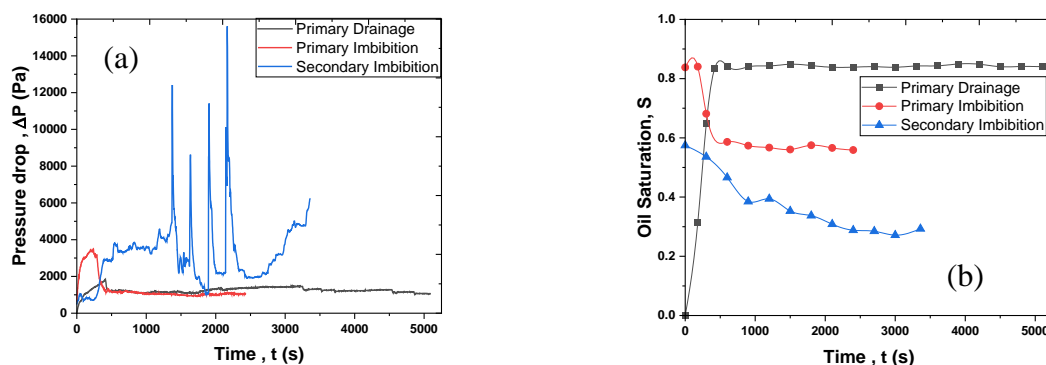


Figure 8. Transient response of (a) pressure drop, and (b) oil saturation, as a function of time. Pickering emulsion of IONPs suspension, $C_{Fe}=0.75\text{g/L}$, was injected at the secondary imbibition step.

Table 3. Summary of results from visualization tests

Displacing fluid in Secondary Imbibition	Primary Drainage* S _o	Primary Imbibition S _o	Secondary Imbibition S _o	⁺ μ _{av} (mPa s)	^{&} κ	^{\$} Cax10 ⁻⁵	Oil recovery efficiency (%)
Pickering emulsion C _{PPH} =3.0g/L	0.87	0.55	0.31	28	1.08	0.98	64.4
Pickering emulsion C _{Fe} =0.25g/L	0.82	0.53	0.18	197	7.58	5.2	78.0
Pickering emulsion C _{Fe} =0.75g/L	0.84	0.56	0.29	47	1.81	1.2	65.5

*Residual oil saturation; ⁺Viscosity of emulsion averaged over a single pore; [&]Viscosity ratio: $\kappa = \frac{\mu_{av}}{\mu_o}$ where $\mu_o = 0.026 \text{ Pa s}$; ^{\$}Capillary number: $Ca = \frac{u_0 \mu_{av}}{\sigma_{ow}}$, σ_{ow} is the aqueous suspension / synthetic oil interfacial tension

4. CONCLUSIONS

IONP suspensions are synthesized and stabilized by mixing ferrous (FeIII) chloride solution with the polyphenol extract of parsley. Visualization tests are performed on a glass-etched pore network to examine the potential of emulsions to enhance the residual oil recovery after a primary drainage / imbibition cycle. It seems that the oil displacement efficiency is maximized when injecting the emulsion ensuring the highest values of viscosity ratio, and capillary number which favour a frontal two-phase flow pattern (Table 3).

Acknowledgements

The research project was supported by the Hellenic Foundation for Research and Innovation (H.F.R.I.) under the “1st Call for H.F.R.I. Research Projects to support Faculty members and Researchers and the procurement of high-cost research equipment” (Project Number: HFRI-FM17-361, acronym: EOR-PNP).

References

- [1] <https://response.restoration.noaa.gov/oil-and-chemical-spills> (accessed March 17,2023).
- [2] <https://www.epa.gov/oil-spills> (accessed March 17,2023).
- [3] Selvaraj R., Pai S., Vinayagam R., Varadavenkatesan T., Kumar P.S., Duc P.A., Rangasamy G., 2022. A recent update on green synthesized iron and iron oxide nanoparticles for environmental applications. *Chemosphere*, 308(2), 1-12.
- [4] Yakasai F., Jaafar M.Z., Bandyopadhyay S., Agi A., Sidek M.A., 2022. Application of iron oxide nanoparticles in oil recovery – A critical review of the properties, formulation, recent advances and prospects. *Journal of Petroleum Science and Engineering*, 208(c), 1-32.

- [5] Fahmy H.M., Mohamed F.M., Marzouq M.H., El-Din Mustafa A.B., Alsoudi A.M., Ali O.A., Mohamed M.A., Mahmoud F.A., 2018. Review of Green Methods of Iron Nanoparticles Synthesis and Applications. *BioNanoScience*, 8, 491–503.
- [6] Sharma T., Kumar G.S., Sangwai J.S., 2015. Comparative effectiveness of production performance of Pickering emulsion stabilized by nanoparticle–surfactant–polymer over surfactant–polymer (SP) flooding for enhanced oil recovery for Brownfield reservoir. *Journal of Petroleum Science and Engineering*, 129, 221-232.
- [7] Bizmark N., Ioannidis M.A., 2015. Effects of Ionic Strength on the Colloidal Stability and Interfacial Assembly of Hydrophobic Ethyl Cellulose Nanoparticles. *Langmuir*, 31, 9282-9289.
- [8] Kumar N., Gaur T., Mandal A., 2017. Characterization of SPN Pickering emulsions for application in enhanced oil recovery. *Journal of Industrial and Engineering Chemistry*, 54, 304-315.
- [9] Lin J., Weng X., Dharmarajan R., Chen Z., 2017. Characterization and reactivity of iron based nanoparticles synthesized by tea extracts under various atmospheres. *Chemosphere*, 169, 413-417.
- [10] Karavasilis M., Tsakiroglou C.D., 2019. Synthesis of aqueous suspensions of zero-valent iron nanoparticles (nZVI) from plant extracts: experimental study and numerical modelling. *Emerging Science Journal* 3(6), 344-360.
- [11] Theodoropoulou M.A., Sygouni V., Karoutsos V., Tsakiroglou C.D., 2005. Relative permeability and capillary pressure functions of porous media as related to the displacement growth pattern. *International Journal of Multiphase Flow*, 31, 1155-1180.
- [12] Geremu M., Tola Y.B., Sualeh A., 2016. Extraction and determination of total polyphenols and antioxidant capacity of red coffee (*Coffea arabica* L.) pulp of wet processing plants. *Chemical and Biological Technologies in Agriculture* 3 (25), 1-6
- [13] Kamath V., Chandra P., Jeppu G.P., 2020. Comparative study of using five different leaf extracts in the green synthesis of iron oxide nanoparticles for removal of arsenic from water. *International Journal of Phytoremediation*, 22, 1278-1294.
- [14] Zhmud, B. 2014. Viscosity blending equations. *Lube Magazine* 121, 22-27.